Orthogonal sample design scheme for two-dimensional synchronous spectroscopy: Application in probing lanthanide ions interactions with organic ligands in solution mixtures

9 **AUTHORS**, INCLUDING:

Kun Huang
Chinese Academy of Sciences
57 PUBLICATIONS 883 CITATIONS

SEE PROFILE

Shaoxuan Liu
Shanghai Jiao Tong University
19 PUBLICATIONS 213 CITATIONS

SEE PROFILE

Ying Zhao
Chinese Academy of Sciences
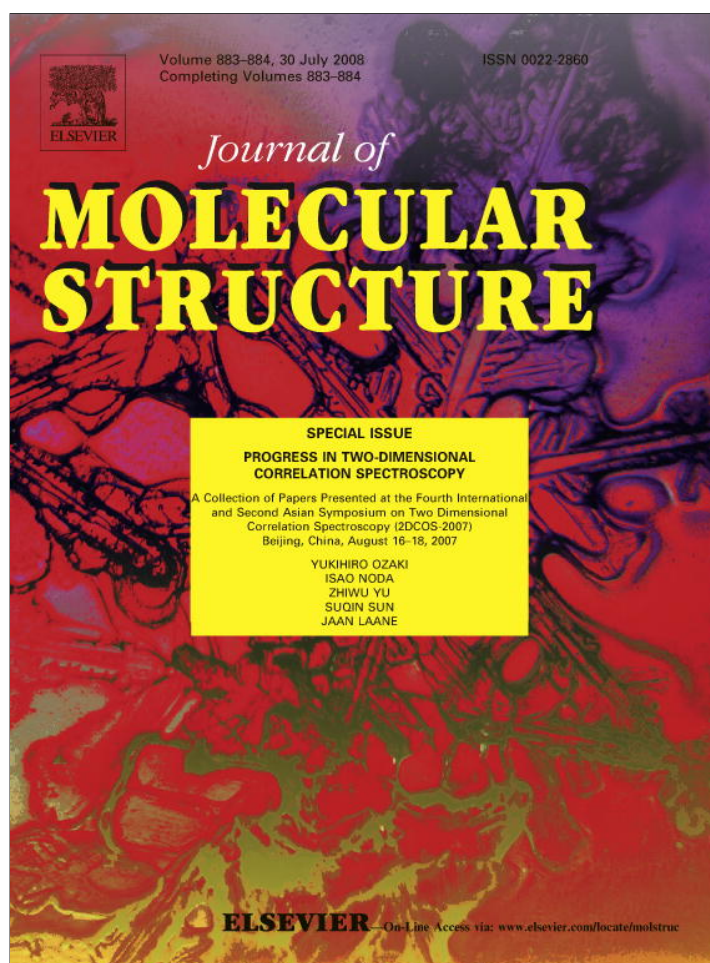97 PUBLICATIONS 1,136 CITATIONS

SEE PROFILE

Isao Noda
University of Delaware
350 PUBLICATIONS 9,236 CITATIONS

SEE PROFILE

Orthogonal sample design scheme for two-dimensional synchronous spectroscopy: Application in probing lanthanide ions interactions with organic ligands in solution mixtures

Jian Qi [a], Kun Huang [a], Xiuxiang Gao [a], Huizhen Li [a,d], Shaoxuan Liu [a], Ying Zhao [b], Yizhuang Xu [a,*], Jinguang Wu [a], Isao Noda [c]

[a] *College of Chemistry and Molecular Engineering, Peking University, Beijing 100871, PR China*
[b] *Institute of Chemistry, Chinese Academy of Sciences, Beijing 100080, PR China*
[c] *The Procter & Gamble Company, West Chester, OH 45069, USA*
[d] *College of Chemistry and Environmental Science, Henan Normal University, Xinxiang 453007, PR China*

Abstract

Weak interactions between lanthanide (III) ions and organic ligands in solution mixtures are studied by using two-dimensional synchronous spectroscopy together with "Orthogonal Sample Design" (OSD) scheme that can effectively remove the interfering cross peaks in 2D synchronous spectrum. Two representative chemical systems are investigated and discussed here: (1) $PrCl_3$/butanone in ethanol solution, where weak coordinative interaction between Pr^{3+} and carbonyl group from butanone is characterized by using 2D UV/IR heterogeneous spectroscopy; and (2) $NdCl_3$/5-sulfosalicylic acid in aqueous solution, where the interaction between Nd^{3+}/5-sulfosalicylic acid is investigated by using 2D UV spectra. The cross peaks occurred in the 2D spectra confirm the weak interactions between lanthanide (III) ions and corresponding molecules where no observable variation occurs in conventional 1D spectra.
© 2008 Elsevier B.V. All rights reserved.

Keywords: Orthogonal sample design scheme; 2D Correlation analysis; Synchronous spectrum; Cross peaks; Intermolecular interaction

1. Introduction

Lanthanide ions (Ln^{3+}) have its 4f orbitals filled with different number of electrons. The 4f electrons confer Ln^{3+} with abundant electronic energy levels and the resultant f–f transitions cover a broad spectral region which ranges from infrared to ultra-violet. Many functional materials based on f–f transitions have been developed such as LEDs [1], immunoassay sensors [2] and biological indicators [3,4]. An important structural feature of Ln^{3+} is that the 4f electrons are efficiently shielded by the closed 5s and 5p shells. Therefore, f–f transitions band are quite sharp, since most influence from ligands environment has been shield by 5s

and 5p orbitals. The effects of ligands that coordinate to the lanthanide ions, albeit subtle, do exist. For example, the interaction between f–f transition and various transitions from ligands may play an important role in energy transfer during the luminescent process of lanthanide complexes. The presence of internal 4f electrons transitions spectra and sensitivities of these transitions towards immediate coordination environment, make spectra involving 4f electrons transitions a powerful tool to investigate the coordinative behavior of Ln^{3+} ions in different ambience [5]. Over the past years, there has been a resurgence of interest in the coordinative behavior of Ln^{3+} ions in solutions particularly in an aqueous medium [6–8]. For example, Carnall gives a critical study of the absorption spectra of Ln^{3+} in solutions [9]. In many cases, however, interactions between lanthanide ions/organic ligands in solutions can only induce subtle spectral variations that are often buried within

complex spectral profiles and are not very easy to be visualized in conventional 1D spectra.

The advent and rapid development of two-dimensional (2D) correlation spectroscopy provides us a new avenue to study intermolecular interactions [10–15]. 2D correlation spectroscopy is a powerful spectral analysis technique based on the analysis of a set of spectral data, which are sequentially obtained under some forms of perturbation applied to the sample. The resultant spectra are transformed into a correlation intensity plot on a spectral plane defined by two independent spectral variable axes [15]. This method is applicable to various spectroscopic experiments, such as FT-IR, FT-Raman, and UV–vis spectroscopy. Many important spectral features that are not readily accessible in the original set of 1D spectra can be clearly visualized in the 2D spectra [16]. 2D correlation spectroscopy has attracted extensive interests for a broad range of applications in a variety of research fields over the past two decades [16–41]. For example, the cross peaks in 2D synchronous spectrum can be used to characterize intermolecular interactions, including dipole–dipole and dipole–π interactions. In principle, the appearance of cross peak in 2D synchronous spectrum may suggest the presence of intermolecular interaction. However, interfering cross peaks due to other sources of synchronicity (accidental synchronicity), such as concentration variations of solutes, also arise even if there is no intermolecular interaction. This problem makes it difficult to directly use the cross peaks in conventional 2D synchronous spectrum as a reliable criterion to judge if intermolecular interaction actually occurs or not.

In our previous work, we propose an orthogonal sample design (OSD) approach to solve the problem, so that intermolecular interaction between two solutes (denoted as P and Q) dissolved in a solution can be characterized under the framework of 2D synchronous spectroscopy using varying concentrations as an external perturbation. In this approach, a series of 1D spectra (1, 2, ..., m) of P/Q mixture with variable concentrations of P and Q (denoted as C_P^i and C_Q^i, respectively) are recorded and used to construct 2D synchronous spectrum by using the algorithm proposed by Noda [16–41]. The selection of the initial concentrations of P and Q should meet the requirement of OSD that is satisfying the following Eq. (1):

$$\sum_{i=1}^{m}(C_P^i - \overline{C}_P)(C_Q^i - \overline{C}_Q) = 0 \qquad (1)$$

Where $\overline{C}_P$ and $\overline{C}_Q$ are the average initial concentrations of P and Q, respectively.

In our previous work [42], we demonstrate that this approach can effectively remove interfering cross peaks caused by accidental synchronicity. As a result, intermolecular interactions, which cause the spectral behavior of the solutes deviate from the Beer–Lambert law in such a subtle manner and can hardly be observed in conventional 1D spectra, can be clearly visualized as cross peaks in 2D synchronous spectrum. This provides a sound basis that allows us to investigate intermolecular interactions in complex chemical systems.

In this paper, we apply the OSD on two chemical systems to characterize the weak interactions between Ln^{3+} ions and organic ligands in solutions. They are as follows:

(i) PrCl$_3$/butanone in ethanol solution, where weak coordinative interaction between Pr^{3+}/C=O group is probed by using 2D heterogeneous UV/FT-IR spectra.

(ii) NdCl$_3$/5-sulfosalicylic acid in aqueous solution, where f–f transition/π–π transition interaction between Nd^{3+}/5-sulfosalicylic acid is investigated by using 2D UV spectra.

2. Experimental

2.1. Materials

Nd$_2$O$_3$ and Pr$_4$O$_{11}$ with purity of 99.99% were purchased from Shanghai Yuelong chemical factory. The lanthanide chlorides were prepared by dissolving the corresponding lanthanide oxides in concentrated HCl. Other chemicals were of A.R. grade and purchased from Beijing Chemical Company.

2.2. Instrument

The FT-IR spectra were collected on a Bio-Rad FTS-65A Fourier transform infrared spectrometer equipped with an attenuated total reflection accessory. All the spectra were recorded at a resolution of 4 cm^{-1} and 32 scans were co-added.

The UV–vis spectra were recorded on a Varian Cary 1E UV–vis spectrophotometer and the spectra were measured at a scanning rate of 60 nm/min.

The 2D synchronous spectra were calculated based on the algorithm by Noda [13,15] using the software of MATLAB (The Math Works Inc.).

2.3. General procedure of constructing 2D mixed solutions synchronous spectrum

We use an example listed in Table 1 to show the general procedures of constructing 2D synchronous spectrum from a chemical system containing solute P and solute Q.

Step (i): Four solutions containing P and Q are prepared, and the concentrations of P and Q (denoted as $_{PQ}C_P^i$, $_{PQ}C_Q^i$, $i = 1, 2, 3, 4$) are set as listed in Table 1. The selection of the concentrations of $_{PQ}C_P^i$, $_{PQ}C_Q^i$ ($i = 1, 2, 3, 4$) meet the requirement of Eq. (1).

Step (ii): Four 1D spectra denoted as a_i ($i = 1, 2, 3, 4$) are recorded for the four solutions obtained in step (i).

Step (iii): A *2D mixed solutions synchronous spectrum* of P/Q is then generated based upon the four 1D spectra

Table 1
An example of orthogonal concentration series and spectral information of P and Q for constructing 2D mixed solutions synchronous spectrum

Spectral No.	Spectral type	C_P^i(or $_{PQ}C_P^i$)	C_Q^i(or $_{PQ}C_Q^i$)	$\widetilde{C}_P^{i\ \text{a}}$	$\widetilde{C}_Q^{i\ \text{a}}$
a_1	1D spectrum of P and Q mixture	5	6	1	0
a_2	1D spectrum of P and Q mixture	4	7	0	1
a_3	1D spectrum of P and Q mixture	3	6	−1	0
a_4	1D spectrum of P and Q mixture	4	5	0	−1
$\overline{C}_P^i(\overline{C}_Q^i)$	1D spectrum of P and Q mixture	4	6	–	–

$^{\text{a}}$ $\widetilde{C}_P^i = C_P^i - \overline{C}_P^i$, $\widetilde{C}_Q^i = C_Q^i - \overline{C}_Q^i$, $i = 1, 2, 3, 4$.

obtained in step (ii). The cross peak at (x, y) in the 2D mixed solutions spectrum can be used to characterize intermolecular interactions between P and Q.

2.4. Other considerations

Before we use the cross peak in the obtained 2D mixed solutions spectrum, other factors that may bring about additional interfering or artifact cross peaks should be considered. Accordingly, appropriate pretreatments are adopted to make sure that the observed cross peaks are not artifact.

2.4.1. Interference caused by solvent–solute interactions

Every chemical system studied here is a solution consisting of solvent and solutes. Although the contribution from the solvent to the characteristic peaks of the solutes could often be safely neglected, some levels of solvent–solute interactions become inevitable, since a solvating layer often occurs around each solute molecule. These interactions may lead to a deviation from linearity between absorbance and concentration of the solutes. Such a deviation may also produce cross peaks that reflect solute–solvent interactions rather than solute–solute interactions.

The following consideration is helpful to remove the potential interference caused by solvent–solute interactions. The solute and its solvating layer can be regarded as an entity called solvated–solute complex. Within a suitable concentration range of the solutes, the integrity of the solvated–solute complex remains virtually undisturbed. The so-called Beer–Lambert law is actually manifested by the solvated–solute complex rather than solute molecule alone. That is to say, intermolecular interactions among solute and solvent do not produce interfering cross peak in 2D synchronous spectrum provide the concentrations of the solute is within a suitable range.

Experimentally, a series of solutions are prepared first by dissolving each solute separately in the corresponding solvent for spectral measurement. Based on the experimental results, we then determine the suitable concentration ranges where good linear relationships between the absorbance of the characteristic peaks and concentrations of the solutes are obtained ($R > 0.99$, see supporting information).

Accordingly, we select the aforementioned concentration ranges to construct 2D synchronous spectra, thereby

excluding the possibility that the cross peaks are caused by solvent–solute interactions.

For comparison, we also consider solutions containing different solute molecules and intermolecular interactions occur among different solutes. In this case, the integrity of the solute–solvent complex cannot exist any longer because of intermolecular interaction among different solutes. As a result, deviation from the Beer–Lambert law occurs and brings about cross peak in 2D synchronous spectrum.

2.4.2. Deviation from the linearity between absorbance and concentrations of the solutes caused by experimental errors

During the process of constructing 2D synchronous spectrum based on our approach, the concentration series of P and Q are selected to make their dynamic concentrations orthogonal to one another. As long as the Beer–Lambert law holds, the dynamic absorbance of P and Q also should become orthogonal to one another.

However, even if good linearity is present between absorbance and concentration, some unintentional deviation from the linearity is often encountered in real-world experiments. Such a deviation might affect the orthogonality of the dynamic absorbance between P and Q and produce interfering cross peaks.

To estimate the effect of such deviation, a 2D negative control spectrum should be generated when cross peaks between the characteristic peaks from P and those from Q appear in 2D synchronous spectrum constructed by our approach. An illustrative example of the procedure for constructing 2D negative control spectrum is given as follows:

Step (i): Four 1D spectra (denoted as b_i, $i = 1, 2, 3, 4$) of P alone dissolved in its solvent are obtained. The concentrations of P in the four spectra (Table 2) are denoted as $_PC_P^i(i = 1, 2, 3, 4)$, where

$$_PC_P^i = {}_{PQ}C_P^i, \quad i = 1, 2, 3, 4 \tag{2}$$

Step (ii): Similarly, four 1D spectra (denoted as c_i, $i = 1, 2, 3, 4$) of Q alone dissolved in its solvent are recorded. The concentrations of Q in the four spectra (Table 2) are denoted as $_QC_Q^i$ ($i = 1, 2, 3, 4$), where

$$_QC_Q^i = {}_{PQ}C_Q^i, \quad i = 1, 2, 3, 4 \tag{3}$$

Table 2
An example of orthogonal concentration series and spectral information of P and Q for constructing 2D negative control synchronous spectrum

Spectral No.	Spectral type	$_P C_P^i$	$_Q C_Q^i$	Spectral addition
b_1	1D spectrum of P in solution	5	0	–
b_2	1D spectrum of P in solution	4	0	–
b_3	1D spectrum of P in solution	3	0	–
b_4	1D spectrum of P in solution	4	0	–
c_1	1D spectrum of Q in solution	0	6	–
c_2	1D spectrum of Q in solution	0	7	–
c_3	1D spectrum of Q in solution	0	6	–
c_4	1D spectrum of Q in solution	0	5	–
d_1	1D spectrum to simulate P and Q mixture	–	–	$b_1 + c_1$
d_2	1D spectrum to simulate P and Q mixture	–	–	$b_2 + c_2$
d_3	1D spectrum to simulate P and Q mixture	–	–	$b_3 + c_3$
d_4	1D spectrum to simulate P and Q mixture	–	–	$b_4 + c_4$

Step (iii): Four 1D spectra (denoted as d_i, $i = 1, 2, 3, 4$) are synthesized by spectral addition to simulate the spectra of virtual mixtures of P and Q (Table 2), where

$$d_i = b_i + c_i, \quad i = 1, 2, 3, 4 \tag{4}$$

Step (iv): Based on the simulated 1D spectra (d_i, $i = 1, 2, 3, 4$), a *2D negative control spectrum* is generated. Since the concentrations of P and Q in d_i series are the same as the corresponding ones in a_i series, the spectral feature brought about by the dynamic concentration series in 2D negative control spectrum bear an analogy with the corresponding 2D mixed solutions spectrum. However, P and Q are never mixed together in d_i series, and the spatial separation precluded any possibility of intermolecular interactions between P and Q in the negative control system. That is to say, no intermolecular interactions occur between P and Q in the negative experiment. In addition, although intermolecular interaction between solute and solvent do occur, it does not produce fake cross peak when the concentrations of P and Q are within suitable ranges. Thus, no cross peak is expected to be observed in negative experiment if the unintentional deviation caused by experimental error is not significant enough. Based on the above, when cross peaks appear in 2D mixed solutions spectrum but absent in 2D negative control spectrum, we can safely say that such cross peaks should indeed be attributed to intermolecular interactions.

3. Results and discussion

3.1. PrCl₃/butanone in ethanol solution

Lanthanide (III) ions are hard Lewis acid and show strong preference for oxygen donor chelating ligands. Thus the carbonyl group from butanone may possess ability to coordinate with lanthanide ions. However, unconjugated ketones are weak ligands and exhibit insignificant spectroscopic changes upon coordinating with metal ions. On the other hand, the 4f electrons of lanthanide (III) ions are generally insensitive to environmental changes, since they are shielded by 5s and 5p electrons. Thus, the interaction between 4f electrons of lanthanide (III) ions and carbonyl group from unconjugated ketone is hardly probed by using conventional spectroscopic methods.

In this experiment, we use PrCl₃/butanone as an example. The f–f transition bands at 446, 470, and 483 nm in UV–vis spectra are used to reflect the variation of 4f electrons of Pr^{3+}, and C=O stretching band at 1709 cm⁻¹ in FT-IR spectra is selected to probe the state of carbonyl group (Fig. 1a or 1b). The hetero-spectral correlation 2D-synchronous plot generated by using the orthogonal sample design is utilized to study this weak interaction during the coordination process.

Fig. 1a depicts the carbonyl stretching bands of butanone dissolved in ethanol. For comparison, a typical carbonyl stretching bands from PrCl₃/butanone mixture dissolved in ethanol is also shown in Fig. 1a. The experimental results demonstrate that no apparent changes in peak position and bandwidth are observed after PrCl₃ and butanone are mixed together. Similarly, the f–f transition bands of Pr^{3+} do not exhibit any observable changes in UV–vis spectra either (Fig. 1b). It is difficult to judge whether interaction between carbonyl group and 4f electrons occurs or not by conventional 1D spectra.

Fig. 2a depicts the UV–vis/FT-IR hetero-spectral 2D mixed solutions synchronous spectrum constructed from a series of 1D spectra of solutions, whose concentrations are listed in Table 3a. Positive cross peaks between the carbonyl band and the f–f transition bands can be observed at (1707 cm⁻¹, 446 nm), (1707 cm⁻¹, 470 nm), and

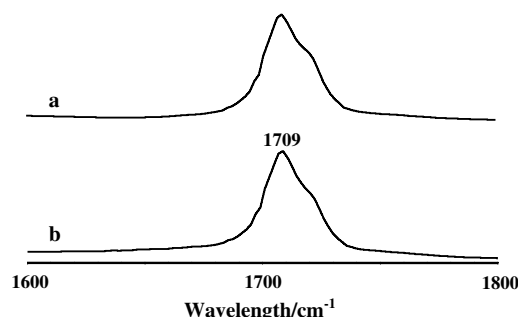Fig. 1a. FT-IR spectra of butanone (a) and PrCl₃/butanone mixture (b) in ethanol solutions. The concentration of butanone is 1.3 mol/L in Fig. 1a.
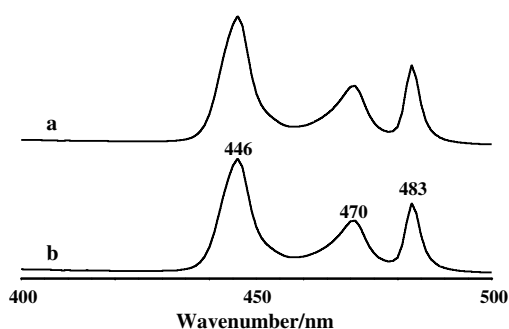
J. Qi et al. / Journal of Molecular Structure 883–884 (2008) 116–123

Fig. 1b. UV–vis spectra of $PrCl_3$ (a) $PrCl_3$/butanone mixture (b) in ethanol solutions. The concentration of Pr^{3+} is 0.075 mol/L in Fig. 1b.
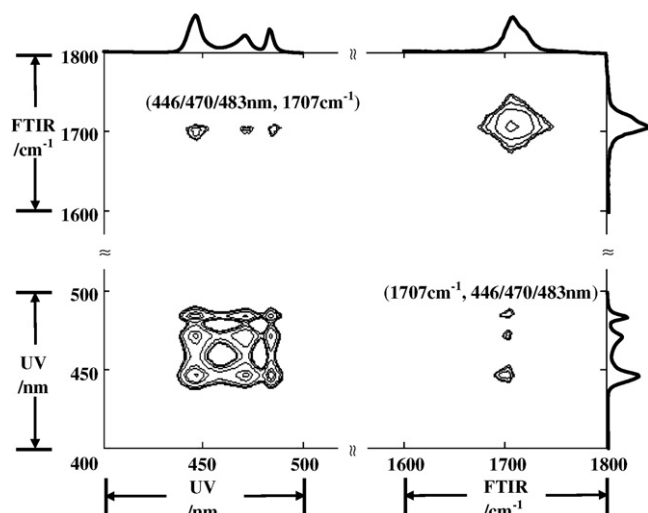

Fig. 2a. 2D mixed solutions synchronous spectrum of $PrCl_3$/butanone system (experimental spectrum). The concentrations of Pr^{3+} and butanone in four solutions are (1) Pr^{3+} 0.075 mol/L, Butanone: 1.3; (2) Pr^{3+} 0.060 mol/L, Butanone: 1.6; (3) Pr^{3+} 0.045 mol/L, Butanone: 1.3; (4) Pr^{3+} 0.060 mol/L, Butanone: 1.1.

Table 3a

Orthogonal concentration series and spectral information for constructing 2D synchronous spectrum (2D mixed solutions spectrum) in Fig. 2a for $PrCl_3$/butanone system

Spectral No.	Spectral type	$PrCl_3$ (mol/L)	Butanone (v/v)	mol/L
A1	1D spectrum of $PrCl_3$/butanone mixture	0.075	12%	1.3
A2	1D spectrum of $PrCl_3$/butanone mixture	0.060	14%	1.6
A3	1D spectrum of $PrCl_3$/butanone mixture	0.045	12%	1.3
A4	1D spectrum of $PrCl_3$/butanone mixture	0.060	10%	1.1

$(1707\ cm^{-1}, 483\ nm)$ in Fig. 2a. The appearance of cross peaks suggests that interaction might have occurred between C=O and 4f electrons of Pr^{3+}.

Before we confirm the existence of interaction based on the presence of the cross peaks, extra steps should be taken to exclude the possibility that the cross peaks are caused by artifacts: (i) Suitable concentration ranges are determined, where good linearity is observed between absorbance and

concentration when either $PrCl_3$ or butanone alone is dissolved in ethanol solution (see supporting information). Thus, the possibility that cross peaks are caused by solute–solvent interaction rather than solute–solute interaction can be excluded. (ii) A negative control experiment (2D negative control spectrum) is conducted to preclude the possibility that cross peaks are caused by experimental errors of dynamic concentration series of the two solutes (Table 3b). The cross peaks at $(1707\ cm^{-1}, 446\ nm)$, and $(1707\ cm^{-1}, 470\ nm)$, $(1707\ cm^{-1}, 483\ nm)$ do not appear anymore in Fig. 2b when $PrCl_3$ and butanone are not in the same solution. That is to say, the presence of the cross peaks in Fig. 2a is indeed a consequence of mixing $PrCl_3$ and butanone.

Based upon the considerations above, we come to the conclusion that the cross peaks in Fig. 2a are caused by the interactions between f-electrons from Pr^{3+} and C=O from butanone. In addition, some interesting spectral features could be found in Fig. 2a. (i) All cross peaks in Fig. 2a are positive, indicating that the interaction between 4f electrons and C=O group made the changes of the dipole moment from f–f transition and C=O vibration in a similar fashion. (ii) In comparison with auto-peak at $(1709\ cm^{-1}, 1709\ cm^{-1})$, the cross peaks at $(1707\ cm^{-1}, 446\ nm)$, $(1707\ cm^{-1}, 470\ nm)$, and $(1707\ cm^{-1}, 483\ nm)$ exhibited observable shift in the frequency of C=O vibration. According to our simulating work [43], we suggest that interaction between Pr^{3+} and butanone brought about

Table 3b

Concentration series and spectral information for constructing 2D negative control spectrum in Fig. 2b for $PrCl_3$/butanone system

| Spectral No.	Spectral type	$PrCl_3$ (mol/L)	Butanone v/v	mol/L	Spectral addition
b_1	1D spectrum of $PrCl_3$ in solution	0.075	0	0	–
b_2	1D spectrum of $PrCl_3$ in solution	0.060	0	0	–
b_3	1D spectrum of $PrCl_3$ in solution	0.045	0	0	–
b_4	1D spectrum of $PrCl_3$ in solution	0.060	0	0	–
c_1	1D spectrum of butanone in solution	0	12%	1.3	–
c_2	1D spectrum of butanone in solution	0	14%	1.6	–
c_3	1D spectrum of butanone in solution	0	12%	1.3	–
c_4	1D spectrum of butanone in solution	0	10%	1.1	–
d_1	1D spectrum to simulate $PrCl_3$/butanone mixture	–	–	–	$b_1 + c_1$
d_2	1D spectrum to simulate $PrCl_3$/butanone mixture	–	–	–	$b_2 + c_2$
d_3	1D spectrum to simulate $PrCl_3$/butanone mixture	–	–	–	$b_3 + c_3$
d_4	1D spectrum to simulate $PrCl_3$/butanone mixture	–	–	–	$b_4 + c_4$
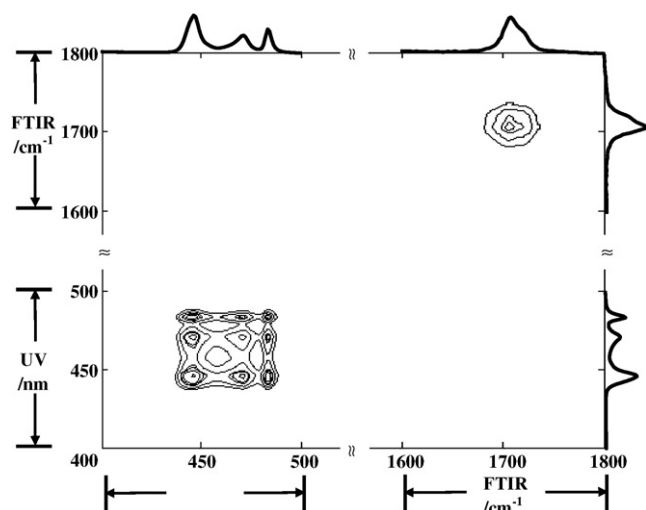
Fig. 2b. 2D negative control synchronous spectrum of $PrCl_3$/butanone system using the concentrations listed in Table 3b (simulated spectrum). The four simulated 1D spectra are: #1:spectrum of 0.075 mol/L Pr^{3+} + spectrum of 1.3 mol/L butanone. #2:spectrum of 0.060 mol/L Pr^{3+} + spectrum of 1.6 mol/L butanone. #3:spectrum of 0.045 mol/L Pr^{3+} + spectrum of 1.3 mol/L butanone. #4:spectrum of 0.060 mol/L Pr^{3+} + spectrum of 1.1 mol/L butanone.

conformational change around C=O group, which might bring about subtle band-shift and variation of bandwidth that is buried by the complex spectral feature in 1D spectra. Further work is obviously necessary to verify this model.

3.2. NdCl₃/5-sulfosalicylic acid in aqueous solution

In this experiment, we use $NdCl_3$/5-sulfosalicylic acid as an example to study the interaction between f–f transition and π–π transition in Nd^{3+}/5-sulfosalicylic acid system. The f–f transition bands at 352, 520, 573, 741, 795, 865 nm in UV–vis spectra are used to reflect the variation of 4f electrons of Nd^{3+}, and π–π transition band at 299 nm in UV spectra is selected to probe the state of phenyl group of 5-sulfosalicylic acid (Fig. 3a or 3b). The 2D-synchronous plot generated by using the orthogonal sample design is used to study this weak interaction during the coordination process.
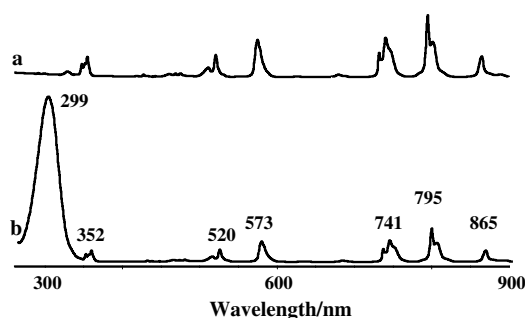

Fig. 3a. UV–vis spectra of $NdCl_3$ (a) and $NdCl_3$/5-sulfosalicylic acid mixture (b) in aqueous solutions. The concentration of Nd^{3+} is 0.024 mol/L in Fig. 1b.
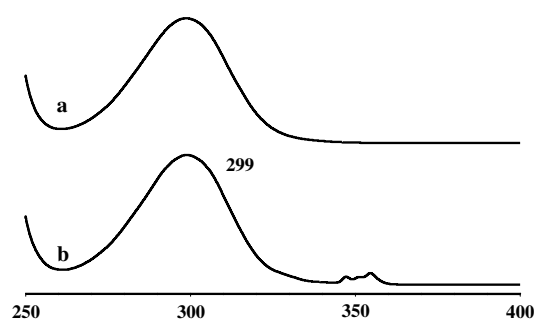

Fig. 3b. UV–vis spectra of 5-Sulfosalicylic acid (a) and $NdCl_3$/5-sulfosal-icylic acid mixture (b) in aqueous solutions The concentration of 5-sulfosalicylic aid is 5×10^{-4} mol/L.

Figs. 3a and 3b depict the UV spectrum of $NdCl_3$/5-sulfosalicylic acid mixture in aqueous solution. The experimental results demonstrate that no apparent changes in peak position and bandwidth are observed after $NdCl_3$ and 5-sulfosalicylic acid are mixed together. It is difficult to judge whether interaction between phenyl ring and 4f electrons occurs or not by conventional 1D spectra.

Fig. 4a depicts the 2D mixed solutions synchronous spectrum constructed from a series of 1D spectra of solutions, whose concentrations are listed in Table 4a. Positive cross peaks between the carbonyl band and the f–f transition bands can be observed at (865 nm, 299 nm), (795 nm, 299 nm), (741 nm, 299 nm) and (573 nm, 299 nm) in Fig. 4a. The appearance of cross peaks suggests that interaction might have occurred between benzyl ring and 4f electrons of Nd^{3+}.

In addition, good linearity is observed between absorbance and concentrations when either $NdCl_3$ or 5-sulfosalicylic acid alone is dissolved in aqueous solution (see
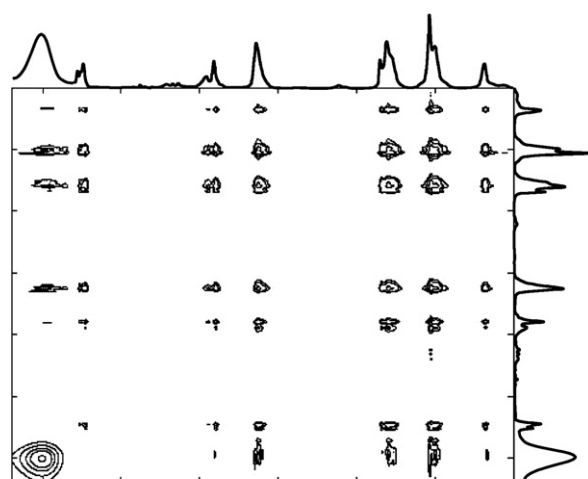

Fig. 4a. 2D mixed solutions synchronous spectrum of $NdCl_3$/5-sulfosal-icylic acid system (experimental spectrum). The concentrations of $NdCl_3$/5-sulfosalicylic acid in the four solutions are (1) Nd^{3+}: 0.024 mol/L, 5-sulfosalicylic acid 5×10^{-4} mol/L. (2) Nd^{3+}: 0.028 mol/L, 5-sulfosalicylic acid 4×10^{-4} mol/L. (3) Nd^{3+}: 0.024 mol/L, 5-sulfosalicylic acid 3×10^{-4} mol/L. (4) Nd^{3+}: 0.020 mol/L, 5-sulfosalicylic acid 4×10^{-4} mol/L.

Table 4a

Orthogonal concentration series and spectral information for constructing 2D mixed solutions synchronous spectrum in Fig. 4a for $NdCl_3$/5-sulfosalicylic acid system

Spectral No.	Spectral type	$NdCl_3$ (mol/L)	5-Sulfosalicylic acid (mol/L)
a_1	1D spectrum of $NdCl_3$/5-sulfosalicylic acid mixture	0.024	5×10^{-4}
a_2	1D spectrum of $NdCl_3$/5-sulfosalicylic acid mixture	0.028	4×10^{-4}
a_3	1D spectrum of $NdCl_3$/5-sulfosalicylic acid mixture	0.024	3×10^{-4}
a_4	1D spectrum of $NdCl_3$/5-sulfosalicylic acid mixture	0.020	4×10^{-4}

Table 4b

Concentration series and spectral information for constructing 2D negative control synchronous spectrum (2D) in Fig. 4b for $NdCl_3$/5-sulfosalicylic acid system

Spectral No.	Spectral type	$NdCl_3$ (mol/L)	5-Sulfosalicylic acid (mol/L)	Spectral addition
b_1	1D spectrum of $NdCl_3$ in solution	0.024	0	–
b_2	1D spectrum of $NdCl_3$ in solution	0.028	0	–
b_3	1D spectrum of $NdCl_3$ in solution	0.024	0	–
b_4	1D spectrum of $NdCl_3$ in solution	0.020	0	–
c_1	1D spectrum of 5-sulfosalicylic acid in solution	0	5×10^{-4}	–
c_2	1D spectrum of 5-sulfosalicylic acid in solution	0	4×10^{-4}	–
c_3	1D spectrum of 5-sulfosalicylic acid in solution	0	3×10^{-4}	–
c_4	1D spectrum of 5-sulfosalicylic acid in solution	0	4×10^{-4}	–
d_1	1D spectrum to simulate $NdCl_3$/5-sulfosalicylic acid mixture	–	–	$b_1 + c_1$
d_2	1D spectrum to simulate $NdCl_3$/5-sulfosalicylic acid mixture	–	–	$b_2 + c_2$
d_3	1D spectrum to simulate $NdCl_3$/5-sulfosalicylic acid mixture	–	–	$b_3 + c_3$
d_4	1D spectrum to simulate $NdCl_3$/5-sulfosalicylic acid mixture	–	–	$b_4 + c_4$

supporting information), thereby excluding the possibility that the cross peaks is caused by solute–solvent interactions. In the 2D negative control spectrum (Table 4b, Fig. 4b), the cross peaks at (865 nm, 299 nm), (795 nm, 299 nm), (741 nm, 299 nm) and (573 nm, 299 nm) do not appear when $NdCl_3$ and 5-sulfosalicylic acid are not in the same solution. The lack of cross peak at (865 nm,

Fig. 4b. 2D negative control synchronous spectrum of $NdCl_3$/5-sulfosalicylic acid system using the concentrations listed in Table 4b (simulated spectrum). The four simulated 1D spectra are: #1:spectrum of 0.024 mol/L Nd^{3+} + spectrum of 5×10^{-4} mol/L 5-sulfosalicylic acid. #2:spectrum of 0.028 mol/L Nd^{3+} + spectrum of 4×10^{-4} mol/L 5-sulfosalicylic acid. #3:spectrum of 0.024 mol/L Nd^{3+} + spectrum of 3×10^{-4} mol/L 5-sulfosalicylic acid. #4:spectrum of 0.020 mol/L Nd^{3+} + spectrum of 4×10^{-4} mol/L 5-sulfosalicylic acid.

299 nm), (795 nm, 299 nm), (741 nm, 299 nm) and (573 nm, 299 nm) in 2D negative control spectrum (Fig.4b) verifies that the dynamic concentration series in Table 4a did not produce interfering cross peaks. Therefore, the cross peaks in Fig. 4a are indeed generated by the f–f transition/π–π transition interaction between the f electrons from Nd^{3+} and π electrons from 5-sulfosalicylic acid.

The above results demonstrate that the cross peaks in Fig. 4a are caused by the interactions between f-electrons from Pr^{3+} and π electrons from 5-sulfosalicylic acid.

4. Conclusion

We apply OSD to probe Ln^{3+} ions weak interactions with organic ligands in two representative chemical systems. The result demonstrates that 2D synchronous spectroscopy, in conjunction with orthogonal sample design scheme, provides us an experimental approach to characterize lanthanide ions/organic ligands interactions.

Appendix A. Supplementary data

Supplementary data associated with this article can be found, in the online version, at doi:10.1016/j.molstruc. 2008.01.036.
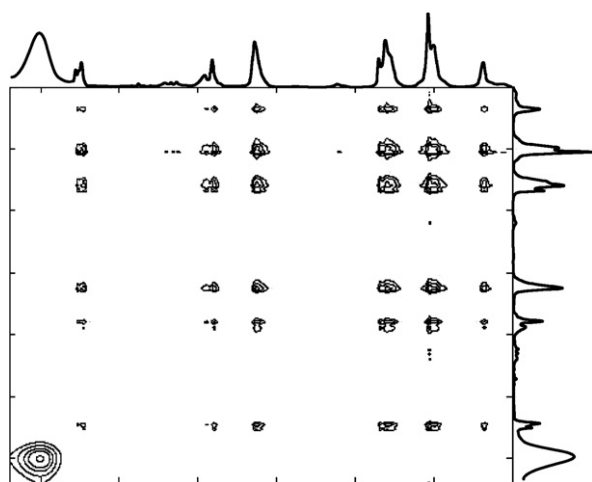
References

[1] R.J. Curry, W.P. Gillin, Curr. Opin. Solid State Mater. Sci. 5 (2001) 481.

[2] T. Lovgren, K. Pettersson, in: K. Van Dyke, R. Van Dyke (Eds.), Luminescence Immunoassay and Molecular Application, vol. 233, CRC Press, Florida, 1990.

[3] X.L. Xu, Q.L. Liu, Y.S. Xie, Biochemistry 41 (2002) 3546.

[4] I. Bertini, I. Gelis, N. Katsaros, C. Luchinat, A. Provenzani, Biochemistry 42 (2003) 8011.

[5] S.N. Misra, G. Ramchandriah, M.A. Gagnani, R.S. Shukla, M.I. Devi, Appl. Spectrosc. Rev. 38 (2003) 433.

[6] A. Bianchi, L. Calabi, F. Corona, S. Fontana, P. Losi, A. Miocchi, L. Paleari, B. Valtancoli, Coord. Chem. Rev. 204 (2000) 309.

[7] E. Toth, L. Burai, A.E. Merbach, Coord. Chem. Rev. 216 (2001) 363.

[8] B.H. Bakker, M. Goes, N. Hoebe, H.J. Ramesdonk, J.W. Verhoeven, M.H.V. Wertz, Coord. Chem. Rev. 208 (2000) 3.

[9] W.T. Carnall, Handbook on Physics and Chemistry of Rare Earths, vol.1, Elsevier, Amsterdam, 1979, Chapter 24.

[10] I. Noda, J. Am. Chem. Soc. 111 (1989) 8116.

[11] I. Noda, Appl. Spectrosc. 44 (1990) 550.

[12] I. Noda, A.E. Dowrey, C. Marcott, Appl. Spectrosc. 47 (1993) 1317.

[13] I. Noda, Appl. Spectrosc. 54 (2000) 994.

[14] W. Zhao, K.M. Murdoch, D.M. Besemann, J.C. Wright, Appl. Spectrosc. 54 (2000) 1000.

[15] I. Noda, Appl. Spectrosc. 47 (1993) 1329.

[16] Y.Z. Ren, M. Shimoyama, T. Ninomiya, I. Noda, Y. Ozaki, J. Phys. Chem. B 103 (1999) 6475.

[17] A. Awichi, E.M. Tee, G. Srikanthan, W. Zhao, Appl. Spectrosc. 56 (2002) 897.

[18] E.M. Tee, A. Awichi, W. Zhao, J. Phys. Chem. A 106 (2002) 6714.

[19] Z.W. Yu, L. Chen, S.Q. Sun, I. Noda, J. Phys. Chem. A 106 (2002) 6683.

[20] Y.W. Wang, W.Y. Gao, I. Noda, Z.W. Yu, J. Mol. Struct. 799 (2006) 28.

[21] J.M. Zhang, H. Sato, H. Tsuji, I. Noda, Y. Ozaki, Macromolecules 38 (2005) 1822.

[22] J.M. Zhang, H. Tsuji, I. Noda, Y. Ozaki, Macromolecules 37 (2004) 6433.

[23] Z.W. Yu, Y.W. Wang, J. Liu, Appl. Spectrosc. 59 (2005) 388.

[24] J.M. Zhang, H. Tsuji, I. Noda, Y. Ozaki, J. Phys. Chem. B 108 (2004) 11514.

[25] J. Liu, Y. Feng, L. Chen, G.S. Wu, Z.W. Yu, Vib. Spectrosc. 36 (2004) 61.

[26] Y.Z. Ren, M. Shimoyama, T. Ninomiya, K. Matsukawa, H. Inoue, I. Noda, Y. Ozaki, J. Phys. Chem. B 103 (1999) 6475.

[27] Y. Ozaki, Y.L. Liu, Macromolecules 30 (1997) 2391.

[28] H.X. Liu, S.Q. Sun, G.H. Lv, Spectrochim. Acta Part A 64 (2006) 321.

[29] Y.M. Jung, B. Czarnik-Matusewicz, Y. Ozaki, J. Phys. Chem. B 104 (2000) 7812.

[30] S.Q. Sun, C.W. Li, J.P. Wei, Q. Zhou, I. Noda, J. Mol. Struct. 799 (2006) 72.

[31] Q. Zhou, S.Q. Sun, L. Yu, C.H. Xu, I. Noda, X.R. Zhang, J. Mol. Struct. 799 (2006) 77.

[32] S. Šašić, A. Muszynski, Y. Ozaki, J. Phys. Chem. A 104 (2000) 6388.

[33] M.A. Czarnecki, B. Czarnik-Matusewicz, Y. Ozaki, M. Iwahashi, J. Phys. Chem. A 104 (2000) 4906.

[34] S. Šašić, A.T. Amari, Y. Ozaki, Anal. Chem. 73 (2001) 5184.

[35] T. Amari, Y. Ozaki, Macromolecules 35 (2002) 8020.

[36] S. Šašić, Y. Ozaki, Anal. Chem. 73 (2001) 2294.

[37] Y.Z. Xu, Y. Zhao, J. Feng, FACSS, Rhode Island (2002) 204.

[38] N. Kang, Y.Z. Xu, W.H. Li, AIP Conference Proceeding, 503 (Two-Dimensional Correlation Spectroscopy), (2000) 245.

[39] Y.Z. Xu, S.F.Weng, W.X. Sun, AIP Conference Proceeding, 503 (Two-Dimensional Correlation Spectroscopy), (2000) 303.

[40] N. Kang, Y.Z. Xu, W.H. Li, J. Mol. Struct. 562 (2001) 19.

[41] B.G. Huang, Y.Z. Xu, S.F. Weng, Chin. Chem. Lett. 13 (2002) 444.

[42] J. Qi, H.Z. Li, K. Huang, H.H. Chen, S.X. Liu, L.M. Yang, Y. Zhao, C.F. Zhang, W.H. Li, J.G. Wu, D.F. Xu, Y.Z. Xu, I. Noda, Appl. Spectrosc. 61 (2007) 1359.

[43] J. Chen, C.F. Zhang, H.Z. Li, Y.Z. Xu, J.G. Wu, I. Noda, J. Mol. Struct., accepted for publication.